Engagement and control of synchroniser mechanisms in dual clutch transmissions

Authors: *Paul D Walker[1], Nong Zhang[1]

Affiliation: [1]Faculty of Engineering and IT, University of Technology, Sydney

15 Broadway, Ultimo, NSW, 2007, Australia

*Corresponding author,

Tel.: +61-2-9514-2987, fax: +61-2-9514-2435

email address: paul.d.walker@eng.uts.edu.au,

Postal address:

University of Technology, Sydney,

PO Box 123

Broadway, NSW, Australia, 2007

Nomenclature

α	–	Cone angle
β	–	Chamfer angle
γ	–	Gear ratio
δ	–	Angular displacement between consecutive chamfers
μ	–	Fluid viscosity
μ_C	–	Dynamic cone friction
$\mu_{C,S}$	–	Static cone friction
μ_I	–	Chamfer friction coefficient
λ	–	Chamfer contact flank
θ_C	–	Excitation system degree of freedom
$\dot{\theta}_S$	–	Cone slip speed
τ	–	Time delay
θ_{FW}	–	Freewheeling component degree of freedom
ω_G	–	Gear speed
$\Delta\omega_{CL}$	–	Clutch slip speed
ΔI	–	Excitation system inertia change
Π	–	Dimensionless group
b	–	Semi-with of contact generatrix in the cone
h	–	Film thickness
t	–	Time
x_S	–	Sleeve displacement
$\dot{x}$	–	Sleeve velocity
A_S	–	Cylinder diameter
C_D	–	Discharge coefficient
C_{RS}	–	Radial clearance
$D_{CV1,2}$	–	Orifice diameter
D_S	–	Cylinder diameter
F_A	–	Axial force
I_{FW}	–	Freewheeling inertia
I_{C0}	–	Excitation system inertia
K_C	–	Excitation system stiffness
P_{CV1}	–	Control volume 1 pressure
P_{CV2}	–	Control volume 2 pressure
P_{EX}	–	Exhaust pressure
P_{IN}	–	Inlet pressure
P_S	–	Solenoid pressure
Q	–	Flow rate
R_C	–	Cone mean radius
R_I	–	Chamfer pitch radius
N_C	–	Number of chamfers
T_B	–	Bearing drag
T_C	–	Cone torque
T_{CL}	–	Clutch drag torque
T_D	–	Drag torque

T_F – Gear tooth friction
T_I – Indexing torque
T_{SH} – Shaft drag torque
T_{syn} – Synchroniser net torque
T_W – Gear windage torque
X_0 – Minimum sleeve displacement for cone contact
X_C – Minimum sleeve displacement for chamfer contact

Abstract

The study of synchroniser engagements in dual clutch transmissions is undertaken in this paper, identifying limitations to the repeatability of actuation, demonstrating one popular solution for positive synchroniser control and offering an alternate engagement tool. Principally, high wet clutch drag and the synchroniser design have lead to detrimental alignments conditions, where indexing chamfers on sleeve and target gear delay engagement of the mechanism and leads to potential sleeve block out. This paper focuses on the investigation into different control methods for overcoming these detrimental alignment conditions. The application of a closed loop control method to overcome block out related engagements is studied, and, for comparison, a novel engagement tool for overriding all chamfer alignment conditions is introduced and evaluated. Results have demonstrated that both techniques have some limitations, with the novel tool being capable of providing direct control of all chamfer engagements with limited extension of the duration of synchroniser engagements, however some tuning of mechanism parameters is required for different engagement conditions.

Keywords: Synchroniser; control; dynamics; gearbox; dual clutch transmission

1. Introduction and background

The dual clutch transmission (DCT) combines technologies of automatic transmissions in the form of hydraulic clutch control with those of manual transmissions, namely gear train and synchronisers. The merger of these two transmission systems in DCTs along with the development of advanced transmission control strategies has seen the rapid development of the DCT as a popular vehicle transmission [1-3]. Extensive research into the shift control dynamics of DCTs has been performed by [4-7] with one common assumption: synchronisation of the target gear for shifting is an independent precursor to gear shifts and therefore does not require investigation. Goetz [6] uses a cone clutch model to simulate the speed synchronisation of the synchroniser, however this does not extend into engagement process of ring unblocking and indexing, which are critical processes for successful engagement, and a source of variation in synchroniser engagement [8,9].

Synchroniser engagement simulations are only considered for manual transmission [10-15]. As such these often include linkages and leavers for driver operation [12], and the engagement is generally controlled by input displacement or velocity to obtain observed force for the driver. Modelling procedures show the high reliance on torque balancing during the engagement process and limited requirements for observation based control techniques. Results demonstrate significant variation in engagement delay depending on alignment, sleeve speed, and common design variables such as friction or cone mean radius. Lui [13] studies chamfer alignment, and along with Hoshino [10] identifies phenomena associated with backward sleeve motion and the beginning of sleeve alignment during indexing, however not the source of this motion is not clearly stated.

The other major consideration is the practicalities of simulating drag torques on the mechanisms. Where [14, 16] identify different drag torques acting on the mechanism and gears, [10, 13] both make no mention of these torques. The dependence of drag on both gear and clutch speeds are crucial to accuracy of models and may change significantly from MTs to DCTs. In Walker [17] the variation in chamfer alignment during hub indexing, the final engagement stage, is highly variable. Initial alignment of chamfers and the generation of slip between sleeve and hub resulting from high drag torque were identified as primary causes to this issue. This can result in variation in engagement of around 10ms, which is significant when the desirable duration of synchroniser engagement is less than 100ms.

Block out is a particular failure mode of synchronisers that results from high drag torque interacting with indexing and cone torques. Where block out results from the inability to achieve speed synchronisation or initiate ring unblocking through drag torque exceeding either of these torques. Further drag torque modelling during the synchronisation process indicates peak drag is realised at speed synchronisation between shaft and gear as a result of high viscous drag in the wet clutch and peak clutch slip speed being achieved at this time [18]. [16,19,20] all have investigated drag torque to some extent, it is generally understood that whilst it is possible to identify and model drag torque, the high level of uncertainty and variability associated with drag torque limits the capacity to influence drag through good transmission design.

This paper will therefore evaluate several techniques for active control of chamfer alignment in synchroniser mechanisms. In the following sections the basics of DCT shifting and synchroniser engagement are reviewed to identify where chamfer alignment

issues fit into DCT control. This is followed by the development of the synchroniser mechanism and hydraulic control system models, including details of how drag torque affects the synchronisation process. Initial simulations are then made to demonstrate the chamfer alignment issue for wet and dry DCTs. Followed by demonstration of current feedback control method for sleeve displacement to provide direct control of re-alignment, and finally an alternative mechanism is suggested and demonstrated to provide direct control of chamfer alignment in DCTs.

1.1. Basic DCT shift process

Figure 1 presents a basic powertrain layout for the DCT, clutches are identified as C1 and C2 with a common drum connected to the engine, and independently engage gears G1 (1^{st}, 3^{rd} or 5^{th} gear) and G2 (R, 2^{nd}, 4^{th} or 6^{th} gear) with synchronisers S1 and S2 locking gears to the output shaft to drive the vehicle.

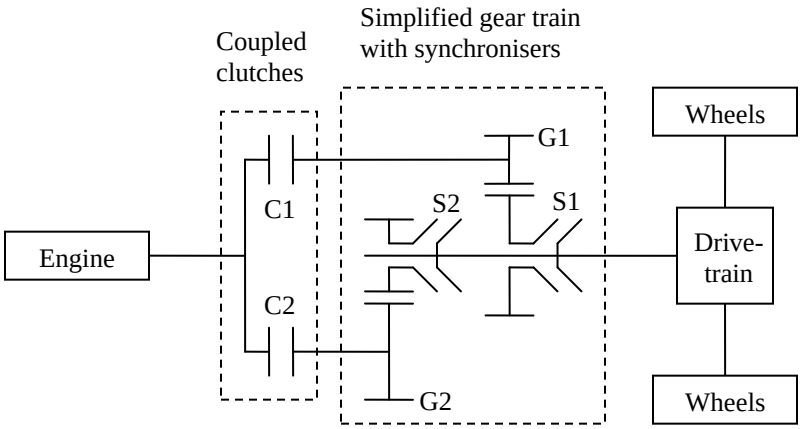

Figure 1: General DCT powertrain layout showing coupled clutches, C1 and C2, and simplified gear train with synchronisers, S1 and S2, and freewheeling gears

To perform a typical up or down shift in the DCT the process begins with synchronising the target gear. Unlike manual transmission this occurs with the engine still driving the

currently engaged gear, and no input from the driver. Linkages for manual transmission, such as those presented in [12], are replaced with electro-hydraulic or electro mechanical controls, see [21, 22], but there are limited opportunities to introduce closed loop control beyond detection of sleeve position. Once the gear is synchronised shifting commences through the simultaneous release and engagement of clutches to transfer power between alternate gear trains. One of the predominant differentiations between synchroniser engagements in the DCT and conventional MTs is that in the DCT the engine speed is maintained at the current gear speed while the synchroniser is engaged, maximising clutch slip speed as synchronisation completes. This result is counter intuitive to [23], identifying reduction in clutch drag as one of the main methods to improve synchroniser performance, whereas it is maximised as speed synchronisation completes in DCTs.

1.2. Synchroniser and synchronisation process

The synchroniser itself and its engagement process are largely unchanged from the introduction of the mechanism from conventional manual transmissions. As shown in Figure 2 the main components are sleeve, with a translational degree of freedom axially along the shaft, ring with limited translational and rotational degrees of freedom, and freewheeling gear and hub with free rotational degree of freedom about the shaft. Chamfers are present internally on the sleeve splines, and externally on ring and hub splines, with the cone clutch external surface on the ring and internal friction surface on the hub.

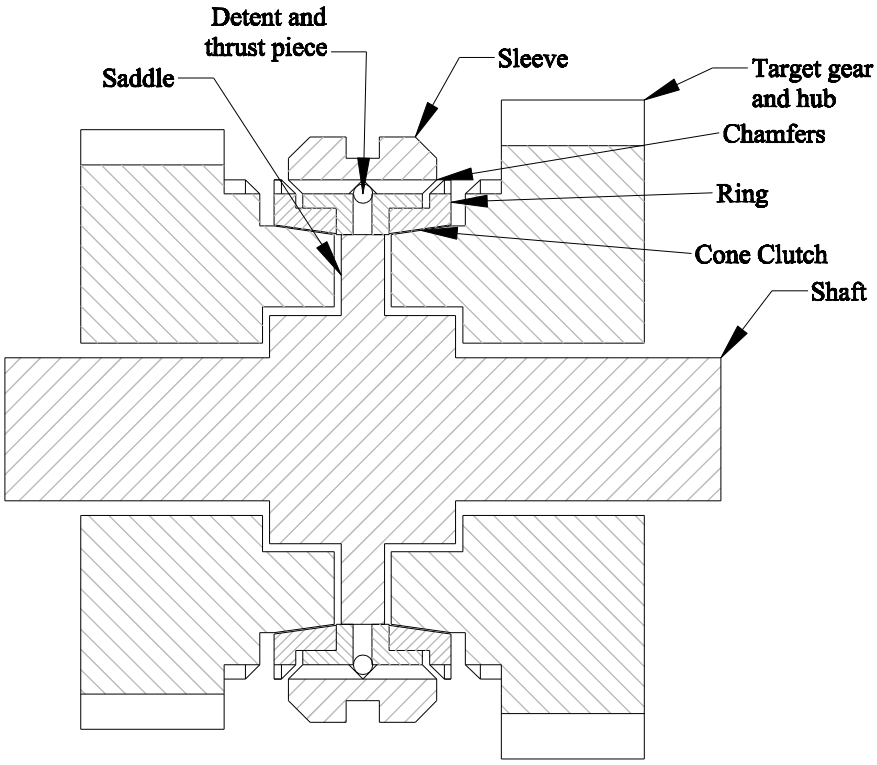

Figure 2: Typical synchroniser mechanism layout with major components shown

The engagement of the synchroniser moves through several different stages as the cone clutch is engaged and the sleeve moves forward with the engagement, locking the gear and shaft in preparation for shifting. Many different process descriptions are available [8, 10, 13, and 14]; with deviations by authors reflecting different research focuses. The process can be outlined in five stages related to sleeve displacement, slip in the cone clutch, and torque balance:

1. Initial displacement – Upon initiation the hydraulic cylinder is pressurised and the sleeve begins to move forward, see Figure 3 (a). Initial resistance to motion is arises from the detents that maintain the neutral position and squeezing oil film from the friction surfaces. This oil film creates a torque between the ring and hub and begins to rotate the ring into the blocking position, where chamfer

blocking torque prevents continued displacement of the hub. This stage ends with oil squeezed from the friction surface and the ring blocking the sleeve.

2. Speed synchronisation – During the entire speed synchronisation process if the cone torque exceeds chamfer torque the sleeve is prevented from moving (Figure 3 (b)), and the friction torque in the cone clutch synchronises speed between the target gear and shaft. Once the speeds are synchronised clutch torque is effectively the combined drag torque and acceleration of the target gear inertia, this signifies the completion of this stage and enables unblocking of the ring.

3. Ring unblocking – When the clutch is synchronised the torque generated at the blocking chamfers on the ring exceeds the clutch torque and allows the sleeve to rotate the ring back to the neutral position as the sleeve again moves forward and continues its engagement. As unblocking completes load is removed from the cone clutch.

4. Secondary displacement – During the secondary displacement the load on the cone clutch is reduced. Thus, as the sleeve moves forward, and if drag on the mechanism is sufficient, it will unlock the cone clutch and cause the regeneration of a relative slip between the target gear and shaft.

5. Hub indexing – The final stage of synchronisation begins with contact between chamfers on the ring and hub, Figure 3 (c) and ends with interlocked splines, Figure 3 (d). The torque generated between these chamfers realigns the hub so that the chamfers slide over the sleeve, completing engagement. Here, engagement is highly dependent on initial chamfer alignment, an entirely random process, and any slip speed in the cone clutch.

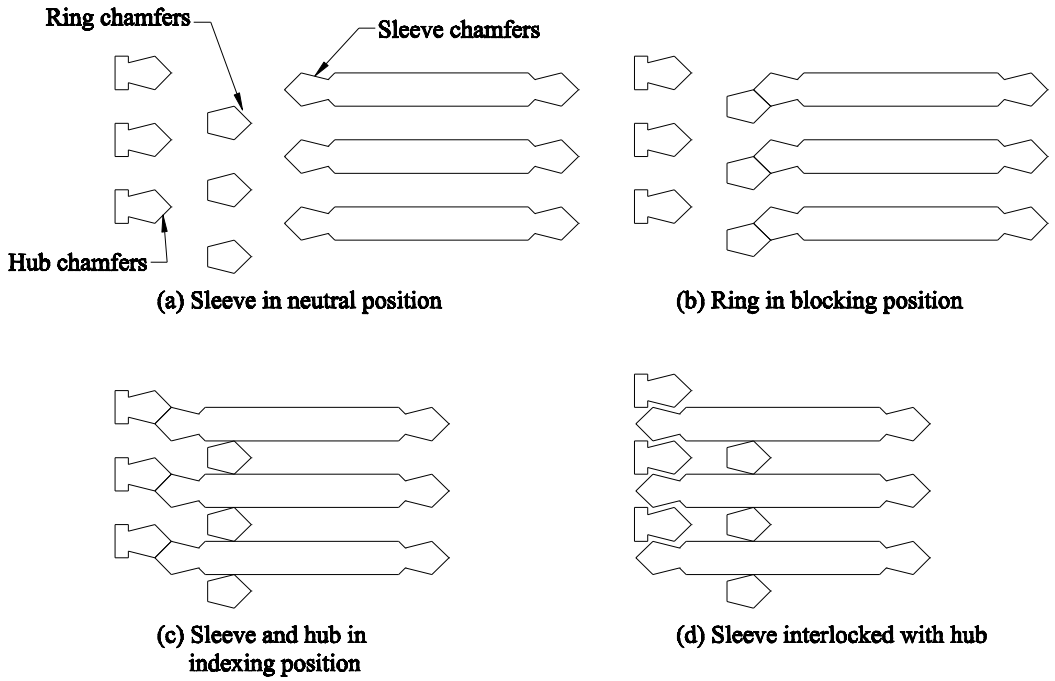

Figure 3: Changes to chamfer alignments during the process of synchronisation

2. Modelling the synchroniser

The synchroniser mechanism relies heavily on the balancing of torques to restrict the displacement of the sleeve and control the engagement of chamfered splines used to interlock the mechanism. Four torques that influence this engagement process are the cone clutch torque, the chamfer torque, for both blocking and indexing, and drag torque [16].

Considering the operating environment of the mechanism, as part of a transmission and vehicle dynamic system modelling the actuation could be complex, requiring powertrain and vehicle models [24]. However, given that the duration of engagement is very short, approximately 100ms, and the inertial of the target gear is significantly smaller than the inertia of the vehicle it is possible to considerably reduce the complexity of the model by

assuming it is a rigid body, and changes in vehicle dynamics will not appreciably influence the process [9]. It is therefore possible to model the synchroniser mechanism as a rigid body with the inertia of all components that are target of synchronisation reflected to the target gear. Thus the model includes the translation displacement of the sleeve as a result of actuation and resisted by chamfer torques, the limited rotation of the ring as it blocks sleeve motion while the cone clutch is energised, and the free rotation of the target gear as it is engaged at the cone clutch and chamfers.

The piecewise cone clutch torque is derived from a viscous contact torque if the clutch is open, a dynamic friction torque for the energised closed clutch with a relative velocity, and the combined acceleration of the target gear and drag torque for the synchronised clutch. This includes a static friction limit for the locked clutch.

$$T_C = \begin{cases} 4\pi\mu R_C^3 b \dfrac{\dot{\theta}_S}{h} & x_S < X_0 \\ \dfrac{\mu_D F_A R_C}{\sin\alpha} & x_S \geq X_0, \dot{\theta} \neq 0 \\ T_D + I_{FW}\ddot{\theta}_S & x_S \geq X_0, \dot{\theta} = 0 \\ \dfrac{\mu_{C,S} F_A R_C}{\sin\alpha} & x_S \geq X_0, \dot{\theta} = 0, T_D > T_C \end{cases} \quad (1)$$

The piecewise clutch model shown above in equation 1 describes the variation in cone clutch torque through the engagement process to the completion of ring unblocking. From the neutral position through to contact of friction surfaces, $x_s < X_0$, viscous contact is present in the cone clutch. Upon contact of friction surfaces and while there is slip in the cone dynamic friction torque is present. Once the speeds have matched cone clutch torque reduces to the net drag and acceleration torques acting on the mechanism, limited by the static friction of the cone clutch such that once broached cone clutch torque

transits back to dynamic friction. This phenomenon is considered as stick-slip in bodies with friction contact.

Chamfer torques at the ring and hub are defined as the circumferential component of the applied load minus a friction loss from the chamfers sliding over each other.

$$T_B = F_A R_I \frac{1-\mu_I \tan\beta}{\mu_I + \tan\beta} \tag{2}$$

This chamfer torque can be arranged specifically for hub indexing [10], considering alignment and relative motion as:

$$T_I = \begin{cases} F_A R_I \dfrac{1-\mu_I \tan\beta}{\mu_I + \tan\beta} & \lambda + ve, \dot{x} + ve \\ F_A R_I \dfrac{1+\mu_I \tan\beta}{\mu_I - \tan\beta} & \lambda + ve, \dot{x} - ve \\ -F_A R_I \dfrac{1+\mu_I \tan\beta}{\mu_I - \tan\beta} & \lambda - ve, \dot{x} + ve \\ -F_A R_I \dfrac{1-\mu_I \tan\beta}{\mu_I + \tan\beta} & \lambda - ve, \dot{x} - ve \end{cases} \tag{3}$$

Throughout the synchronisation process specific conditions for torque balancing must be met, see Figure 5 for definition of contact flank parameter (λ). During speed synchronisation there is a very specific torque balance required to prevent early unblocking of the mechanism, while permitting synchronisation.

$$T_D \leq T_I \leq T_C \tag{4}$$

During ring unblocking, however, the cone – blocking torque relationship must be reversed, resulting from the locking of the cone clutch:

$$T_D \leq T_I > T_C \tag{5}$$

Finally, to maintain synchronisation of the gear during secondary displacement it is required that:

$$T_D \leq T_C \tag{6}$$

This final result is generally difficult to maintain and the load on the cone clutch is significantly reduced, but drag torque is maintained.

Drag torque models include resistance torques from bearings, gears, in the form of windage and friction, [19, 20] in the concentrically aligned primary shafts, and in the wet clutch pack [16]. For the DCT in particular resistances as split into groups associated with the absolute speed of the target gear, from gears and bearings, and those linked to the relative speed in the clutches, notably shaft, bearing, and clutch viscous losses. Speed dependency of these torques result in the summation of drag in an arithmetically as part of the synchroniser mechanism model during the engagement transient.

$$T_D = -sign(\omega_G)(T_W + T_F + T_B) - sign(\Delta\omega_{CL})(T_{CL} + T_{SH} + T_B) \tag{7}$$

This model is only accurate for wet clutch drag, more recently dry clutch DCTs have become prevalent in light torque load vehicles [21, 25]. To further expand these results to the demonstration of dry clutch DCT results it is possible to very simply eliminate the clutch viscous losses from calculations. Though not completely accurate, as there are some losses resulting from the open clutch, it is representative of the dry clutch DCT with the lower drag losses. Equation 7 can be then written for a dry clutch DCT as:

$$T_D = -sign(\omega_G)(T_W + T_F + T_B) - sign(\Delta\omega_{CL})(T_{SH} + T_B) \tag{8}$$

2.1. Hydraulic control system model

The control system for synchroniser engagements is generally simple, using high flow on/off solenoids to actuate paired pistons, moving the synchroniser sleeve to engage one of two synchronisers, arranged in a similar manner to Figure 3. These solenoids provide

high flow and low controller demand to achieve engagement in approximately 100ms. To model the actuating solenoids a separate assumption is made that enables significant reduction in computational requirements. For on/off type solenoids there are only two positions, open to the exhaust or open to the feed line and unlike fluid throttling solenoids there are no settling requirements for the pressure flow as it changes between open orifices. Thus it is reasonable to simplify the valve to a step input upon actuation. There is however the requirement to include the time delays response of the solenoid with the inclusion of the return spring in the mechanism, therefore the on/off actuation solenoids can be modelled thus:

$$P_S = \begin{cases} P_{EX} & Idle \\ P_{IN}\left(1 - e^{(-t/\tau)}\right) & Engaged \end{cases} \tag{9}$$

The flow from each of these solenoids is used pressurise a cylinder and apply load onto the synchroniser mechanism through the piston head. As each synchroniser can move forward or backward to engage different gears there is an additional unactuated cylinder that resists engagement. The arrangement is presented in Figure 4.

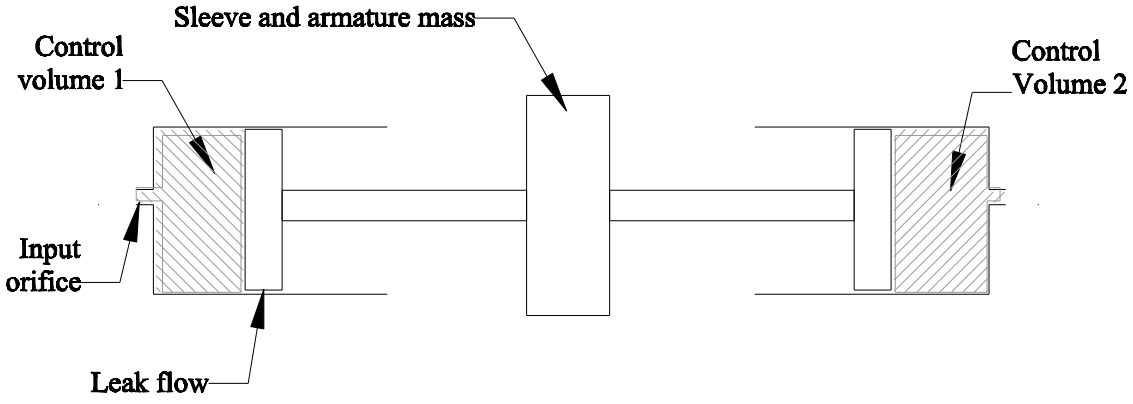

Figure 4: Piston cylinder arrangement for synchroniser actuation, showing flow restrictions from orifice and seal leakage, control volumes 1 and 2, and synchroniser and armature mass.

To develop the pressure model of the two hydraulic cylinders presented in Figure 4, begin with the differential equation of a compressible fluid and apply popular hydraulic theory found in [26-28], see Appendix A for formulation of equations.

$$P_{CV1} = \int \frac{\beta}{V_0 + dV} \left(C_D \pi \frac{D_{CV1}{}^2}{4} \sqrt{P_S - P_{CV1}} - A_S \frac{dX_S}{dt} - C_D \pi D_S c_{RS} \sqrt{P_{CV1} - P_{EX}} \right) dt \qquad (10)$$

$$P_{CV2} = \int \frac{\beta}{V_0 + dV} \left(C_D \pi \frac{D_{CV2}{}^2}{4} \sqrt{P_S - P_{CV2}} + A_S \frac{dX_S}{dt} - C_D \pi D_S c_{RS} \sqrt{P_{CV2} - P_{EX}} \right) dt \qquad (11)$$

To therefore actuate any given synchroniser mechanism a step input control current can be used. This switches the solenoid from the low to the high position, and pressurises and engages the cylinder. As the activated cylinder fills and pressurises according to input from equation 11, the idle cylinder reacts and as hydraulic fluid is squeezed out of the mechanism there will be some pressure build up. Therefore the cylinder arrangement is a reactive load to the engaging mechanism, and will react to the sleeve response.

2.2. Chamfer alignment control using sleeve position

Basic operation of the synchroniser relies on open loop control, where hydraulic load is placed on the mechanism and cone clutch and chamfer torques are relied on to rapidly engage the mechanism. This is limited by alignment conditions that present at the hub, where relative speed and chamfer torque oppose to delay engagement. An alternative technique that is commonly used requires only limited closed loop control of the synchroniser mechanism to track the sleeve displacement as it engages the indexing chamfers and identify conditions that indicate detrimental engagement to initiate override of the engagement, see [29]. Figure 5 demonstrates the simplified algorithm for the override method where the controller identifies if sleeve displacement has reached the

contact zone with the hub chamfers and then detects either the stopping or reversal of the sleeve displacement, both of which indicate a detrimental engagement of the mechanism. If these conditions are detected the controller is triggered and overrides hydraulic control. The idle cylinder is pressurised and control cylinder released to rapidly push the sleeve backwards and allow the chamfers time to re-align. This technique is demonstrated through simulations using ideal input pressures when overriding the engagement control; providing the ideal engagement with minimal time delay.

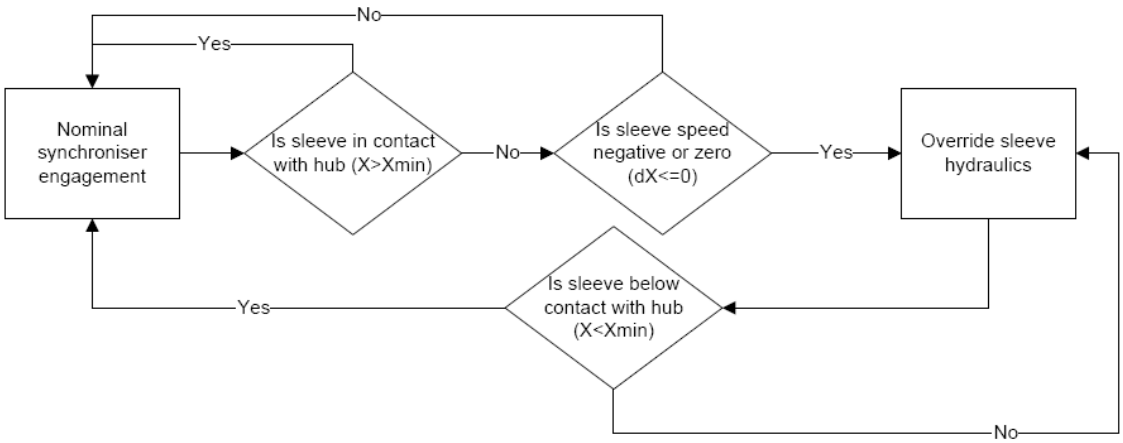

Figure 5: Chamfer override control algorithm

3. A novel tool for direct control of chamfer alignment

The application of closed loop control described in Section 2.2 assumes that poor chamfer engagement will not reoccur when the mechanism is re-engaged. Furthermore delay in engagement will ensue as the sleeve must be pushed back and re-engaged. Thus concluding that application of this direct control does not improve engagement, but provides a measure of certainty that a negative engagement will be overruled and not interrupt gear shift. It is suggested here that a simple inertia change can provide an excitation torque that can provide torsional excitation to aid realignment of chamfers.

Such a variation is conceptually similar to a speed governor; however instead of speed dictating the inertia increase the inertia change is initiated only at the beginning of hub indexing through control of the inertia change. The essentially step change in inertia initiates oscillations in the synchroniser and target gear, generating relative rotational motion between sleeve and hub thereby aiding realignment. To demonstrate the effect of such a model the mechanism model introduced above is modified to include a secondary variable inertia, shown schematically in Figure 6.

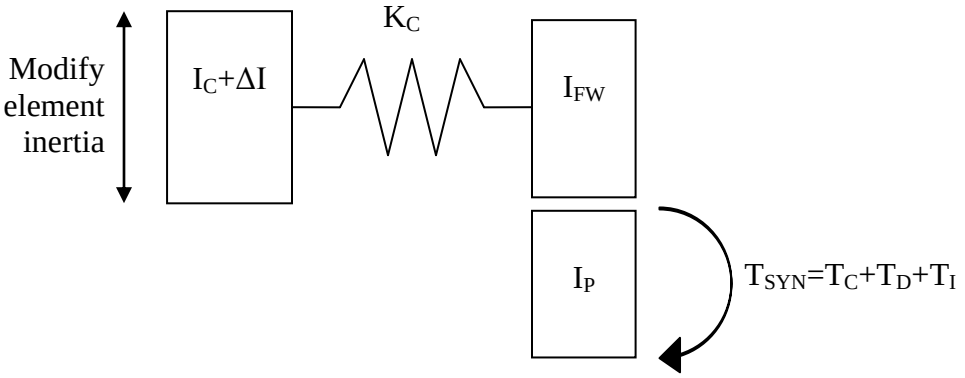

Figure 6: Example model of Inertia change system

This simple two degree of freedom lumped mass system with a reduction gear pair is introduced in equation 12 for simulations using a simple inertia change, modelled as a step change at the initiation of hub indexing, shown in equation 13.

$$\begin{bmatrix} I_C & 0 \\ 0 & \gamma^2 I_{FW}+I_P \end{bmatrix} \begin{Bmatrix} \ddot{\theta}_C \\ \ddot{\theta}_P \end{Bmatrix} - \begin{bmatrix} K_C & -\gamma K_C \\ -\gamma K_C & \gamma^2 K_C \end{bmatrix} \begin{Bmatrix} \theta_C \\ \theta_P \end{Bmatrix} = \begin{Bmatrix} 0 \\ T_{SYN} \end{Bmatrix} \quad (12)$$

The inertia I_C, must be considered as a step response, using:

$$I_C = \begin{cases} I_{C0} & X_S < X_C \\ I_{C0} + \Delta I & X_S \geq X_C \end{cases} \quad (13)$$

To determine the stiffness and inertia parameters for the excitation tool undamped free vibration using equation 12 is conducted, see Rao [30] for free vibration analysis of a

semi-definite system. It is assumed that the natural frequency and amplitude ratio for the semi-definite system are known, and from this data the stiffness, K_C, and damping, I_C, are determined. The natural frequency is chosen such that peak displacement is realised at the end of indexing, such that the average indexing time of 5~10ms is one quarter of the natural period, a frequency range of 25 to 200Hz. The amplitude ratio is chosen to ensure good transmissibility of response without over sizing the inertia and stiffness parameters. Model parameters are shown in Table 1.

Table 1: Simulation model properties for inertia change excitation method

	Stiffness (Nm/rad)	***Initial inertia (Kg-m^2)***	***Final inertia (Kg-m^2)***
Wet	825	0.0001	0.02
Dry	1000	0.0001	0.06

4. Simulations and analysis

Simulation of detrimental engagement of the synchroniser is directly related to the uncontrolled variable of chamfer alignment during the final phase of the synchronisation process; different alignments are demonstrated in Figure 7. In Walker [17] it was demonstrated that, firstly, the cone clutch cannot maintain synchronisation after unblocking of the ring, and secondly, if there is a detrimental chamfer alignment, where the regenerated slip is of the opposing direction to the chamfer torque that the indexing chamfers must first regain the synchronisation by slowing the target gear again before the chamfers can move forward and achieve interlock. Additionally, if there are the conditions of chamfer tips coming into tip-on-tip contact, there is the condition that drag torque must realign the mechanism before engagement begins. The conditions studied

here contribute to partial block out of the synchroniser sleeve during indexing, for high drag conditions this can delay successful engagement, generally identified as hard shifting in manual transmissions [9].

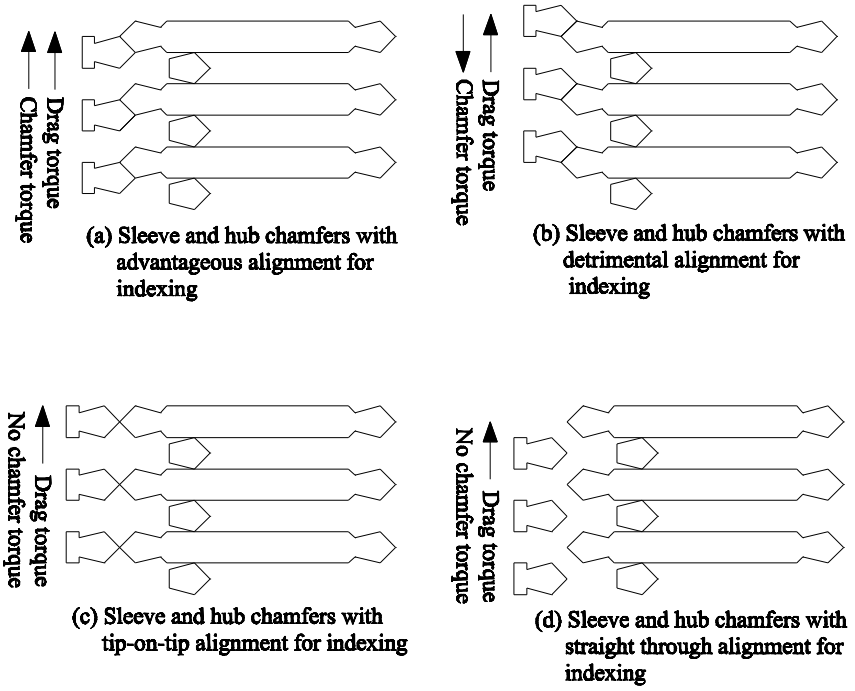

Figure 7: Different cases for chamfer alignments during indexing, (a) is considered negative contact flank, λ, and (b) positive contact flank

The first series of simulations is for the wet clutch DCT, with a combination of chamfer alignments for both up and down shifts used to demonstrate these engagement results. The second group of simulations is for the dry clutch DCT, again with different alignments and for up and down shifts. Two parameters are defined; θ_H is the relative rotation between chamfers on the hub and sleeve and its maximum rotation between two consecutive chamfers, δ. Where $\delta = 2\pi/N_C$, and N_C is the number of chamfers on the sleeve. Model parameters are shown in Table 2:

Table 2: Synchroniser model parameters for simulations

Parameter	*Gear 4*	*Parameter*	*Gear 4*
Gear ratio	1.08	**Cone friction**	0.12
Reflected inertia (kg-m^2)	0.0091	**Chamfer radius (mm)**	60
Number of cones	1	**Chamfer angle (deg)**	65
Cone radius (mm)	47.5	**Chamfer friction**	0.04
Cone angle (deg)	7	-	-

4.1. Simulation of engagement issue

To demonstrate the variation in engagement time as the chamfer alignment changes simulations of a fourth gear synchronisation are conducted with third gear engaged in the transmission. The results shown in Figure 8 indicate that an alignment less than $\delta/2$ provides chamfer realignment duration of less than half that for cases where $\theta_H > \delta/2$.

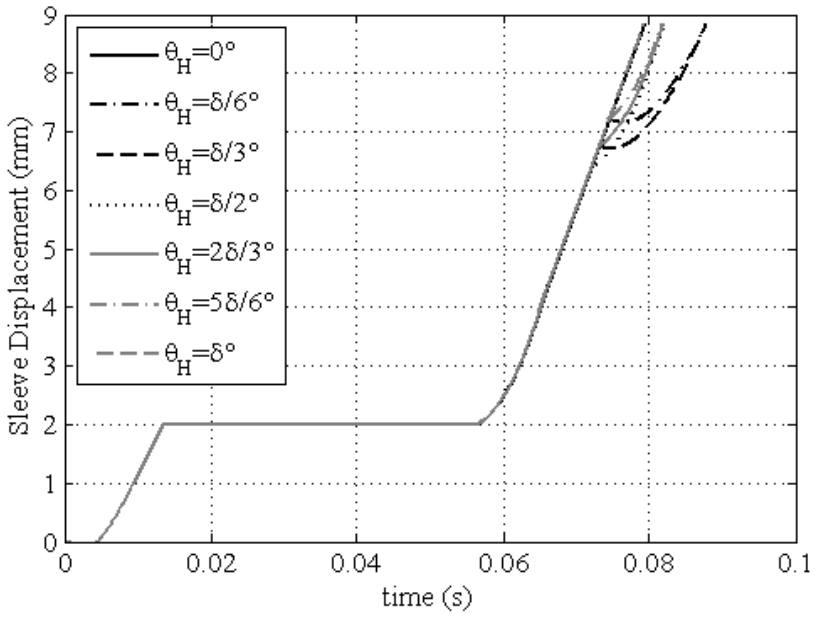

Figure 8: influence of sleeve and gear hub chamfer alignment on synchroniser engagement

4.2. Comparison of different control strategies for wet clutch model

Simulations for different synchroniser control strategies presented in Sections 2 and 3 are conducted for the engagement of fourth gear with third and fifth gears engaged in the transmission.

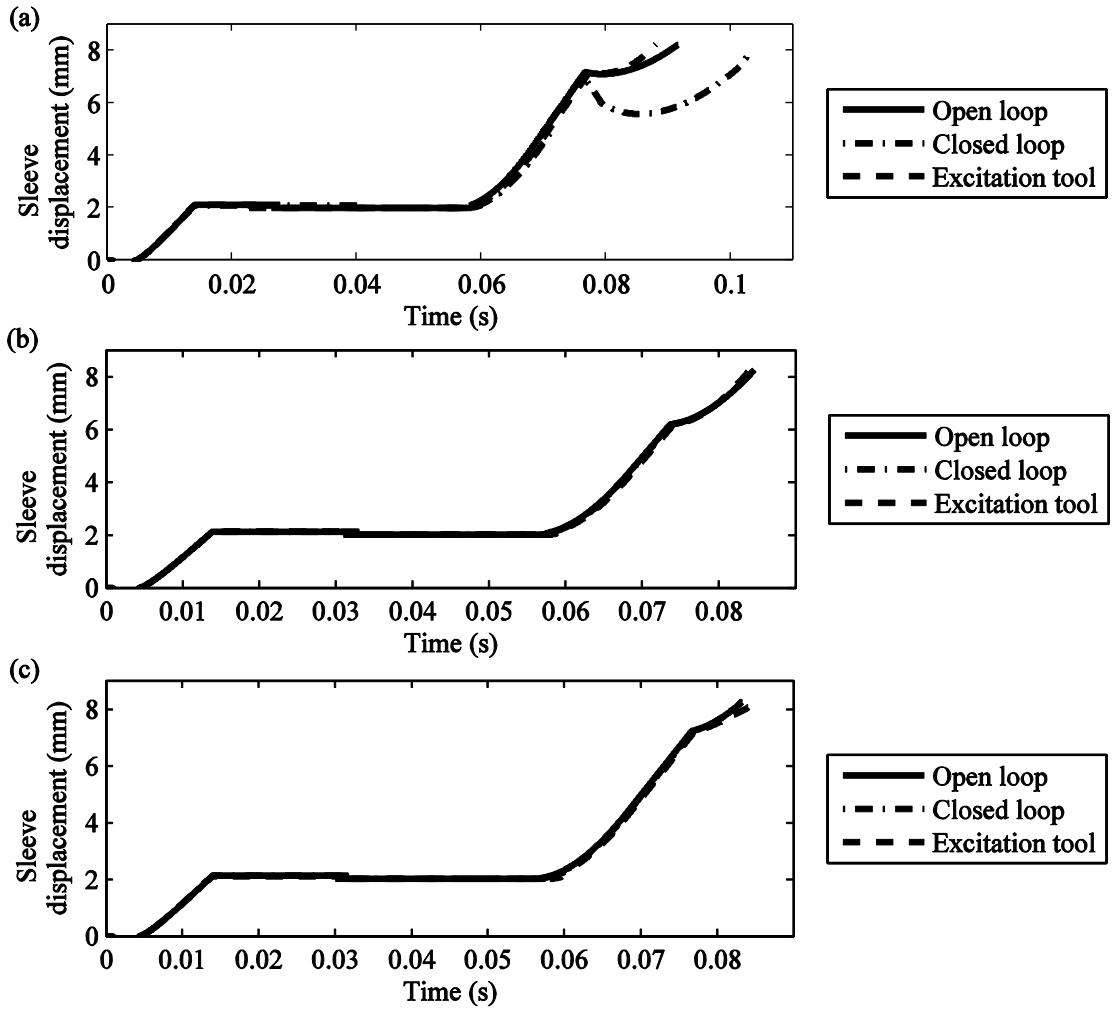

Figure 9: Simulations of different control strategies for synchronisation of fourth gear with third gear engaged in the transmission, with (a) $\theta_H < \delta/2$,(b) $\theta_H = \delta/2$, and (c) $\theta_H > \delta/2$

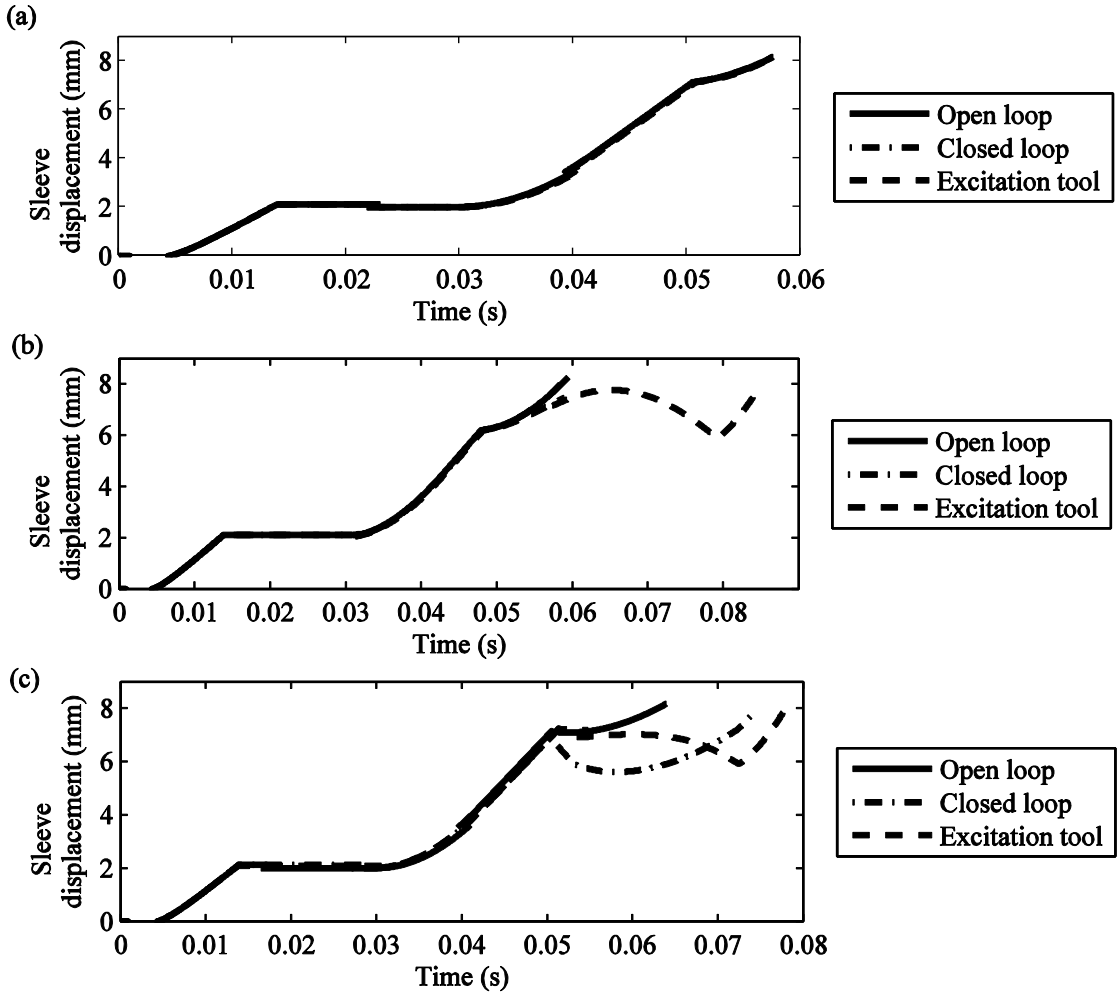

Figure 10: Simulations of different control strategies for synchronisation of fourth gear with fifth gear engaged in the transmission, with (a) $\theta_H < \delta/2$,(b) $\theta_H = \delta/2$, and (c) $\theta_H > \delta/2$

The simulations in Figure 6 present the variation of alignment in the synchroniser mechanism in a wet clutch DCT for up and down shift preparation, targeting fourth gear. Focusing on the post ring unblocking period, the design of the mechanism results in no load on the cone clutch, and as consequence of high drag torques, predominantly from the wet clutch, is the introduction of slip into the mechanism. For both results in figure 6 negative chamfer alignments, see figure 5 (b), results in the significant increase of delay

in indexing of the target gear. Thus for up shift synchronisations when $\theta_H < \delta/2$ indexing is delayed by 10ms, whereas for downshift synchronisations $\theta_H > \delta/2$ for a similar result. The chamfer torque must first brake the regenerated slip speed before indexing can be properly initiated. Furthermore under detrimental alignment drag and chamfer torques partially cancels out, reducing the effectiveness of chamfer torque. The effect of detrimental engagement equates to roughly a 10% variation in the engagement time.

Application of chamfer alignment control of the synchroniser in Figure 9 demonstrates successful application of the control method for the negative chamfer alignment condition in the uncontrolled simulation results presented in Figure 6. With override control triggered the idle cylinder is pressurised and active pressure released between 0.07 and 0.08 seconds. The results demonstrate that once the conditions consistent with restricted engagement are present the sleeve is forced back to completely disengage the hub before being successfully re-engaged. With the higher chamfer alignment the sleeve has to move back further to allow the chamfers' alignment to change significantly. At the low point of engagement there is a delay as the pressures are released in the second cylinder and the active cylinder is again pressurised. Beyond this there is positive engagement of the mechanism. Overall, the engagement is extended by roughly 20 ms or more over the two successful engagements.

The initial simulations, Figure 12, show somewhat contradictory results, for the up shift synchronisation (top), with higher drag torque, the engagement is decreased, where for positive and tip-on-tip alignments the torsion applied to the mechanism rapidly increases engagement. For the negative engagement the torsional excitation rapidly forces the

sleeve backwards as the inertia rotates the synchroniser to the good alignment condition. For the downshift synchronisation (bottom) the results are far less successful, for the tip-on-tip alignment, $\theta_H=\delta/2$, the mechanism is almost successful in engaging the synchroniser, but the vibration becomes negative compared to the chamfer torque and pulls the sleeve back before it climbs over the chamfer tip and engages the sleeve on the advantageous alignment flank. Similarly with $\theta_H>\delta/2$, the detrimental alignment is counterbalanced by the introduced load before forcing the sleeve into advantageous alignment condition. Conversely, the advantageous alignment condition results in the indexing of the hub being reduced similarly to the up shift simulations. The significant change here is the application of drag torque, the drag for the downshift synchronisation being less that for the up shift, indicating that it is necessary to tune the inertia change for different synchronisation scenarios.

4.3. Comparison of different control strategies for dry clutch model

In this section the same simulations as carried out in Section 4.3 are conducted with the application of dry clutch drag torque, as indicated in equation 8. These results are shown in figures 11 and 12 for fourth gear synchronisations with third and fifth gears engaged,

respectively.

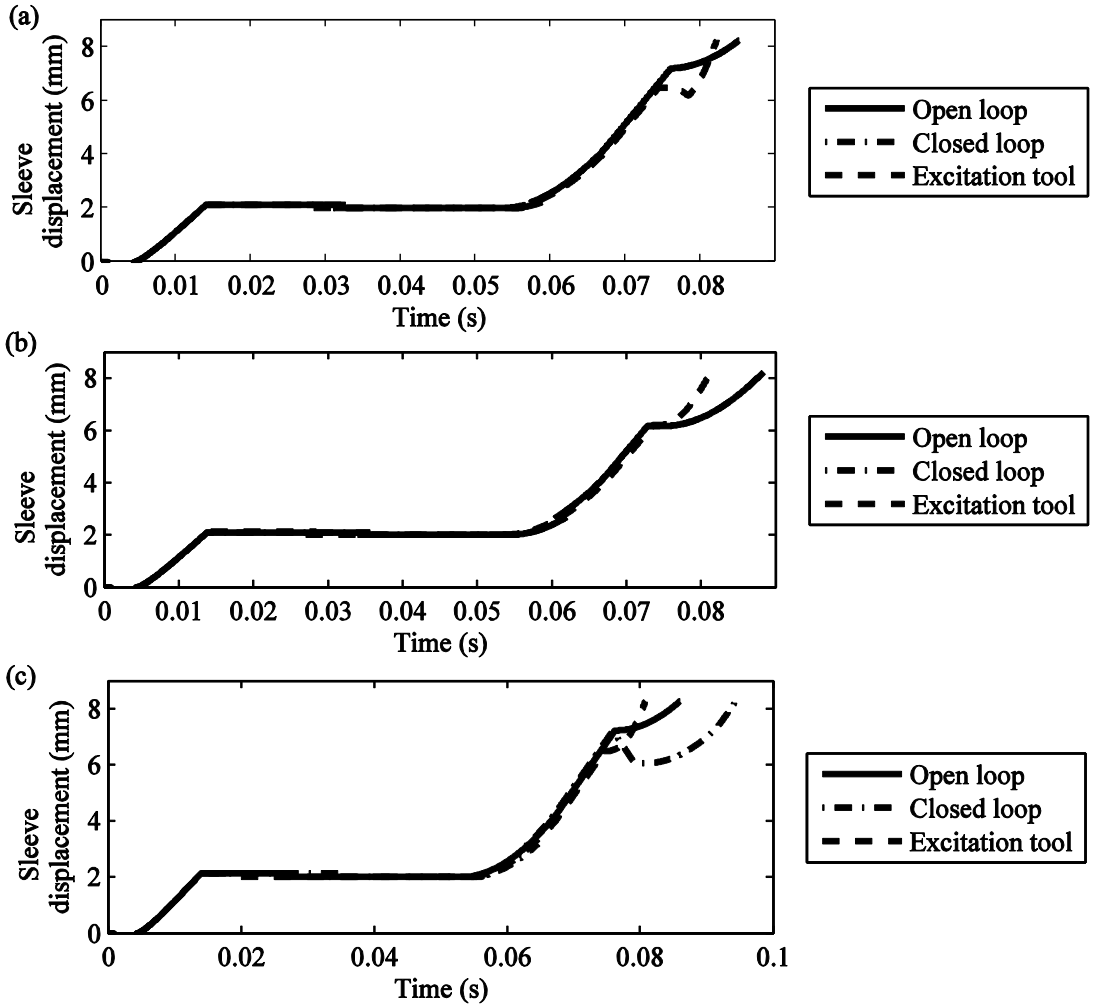

Figure 11: Simulations of different control strategies for synchronisation of fourth gear with third gear engaged in the transmission, with (a) $\theta_H < \delta/2$,(b) $\theta_H = \delta/2$, and (c) $\theta_H > \delta/2$

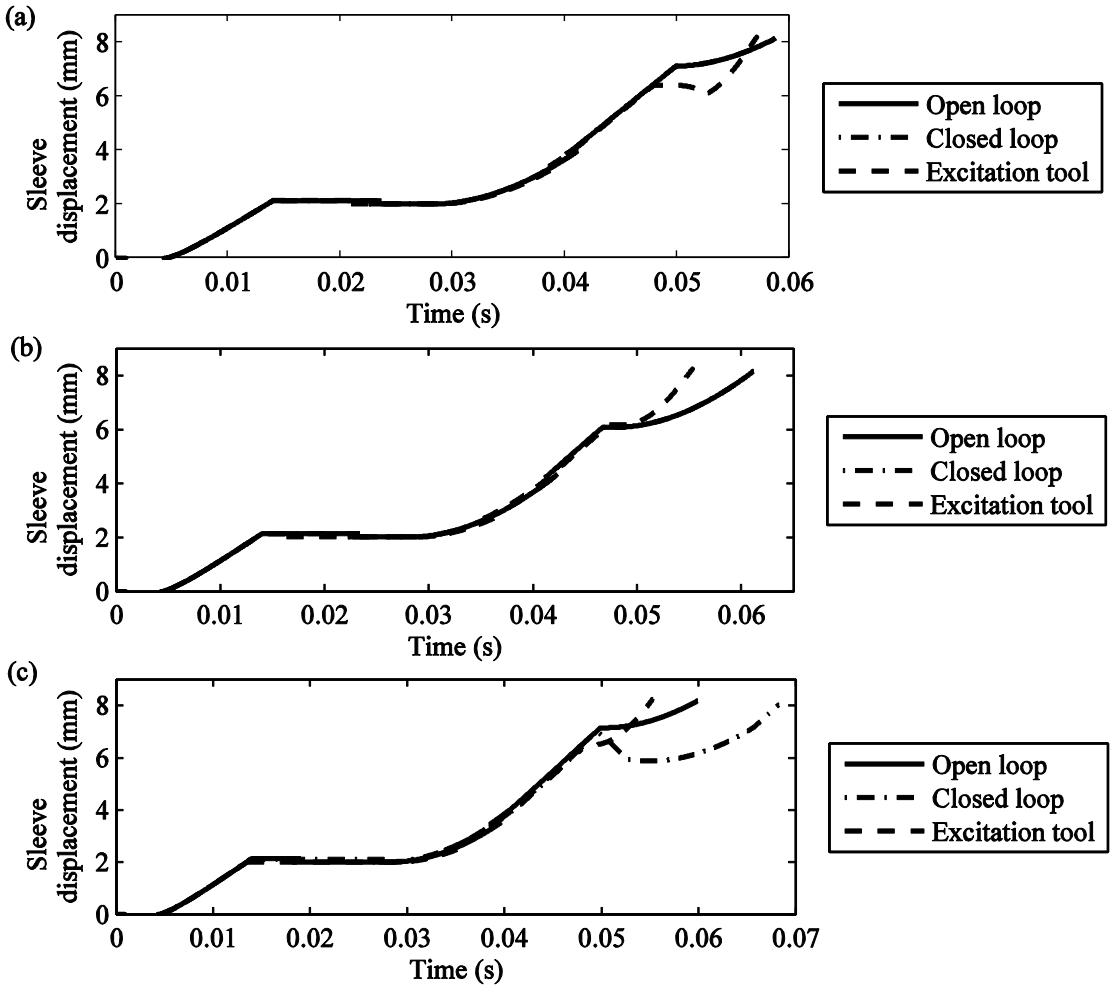

Figure 12: Simulations of different control strategies for synchronisation of fourth gear with fifth gear engaged in the transmission, with (a) $\theta_H < \delta/2$,(b) $\theta_H = \delta/2$, and (c) $\theta_H > \delta/2$

Figure 7 indicates a different result comparing wet and dry clutch simulations. The net drag torque is significantly reduced without the wet clutch, equating to 8 to 10Nm reduction in drag, the post ring unblocking introduction of slip is far less significant, and variation between the chamfer clank alignments is reduced. A separate issue arises in the tip-on-tip condition, $\theta_H = \delta/2$, where a lack of significant drag torques delays the alignment of sleeve and hub to chamfer contact. Given the drag torque model in equation

8, where it is possible for component drags of similar magnitude to cancel each other out, it is possible to extrapolate from these results that tip-on-tip engagement can result a perceived block out event induced from this particular engagement.

The results in Figure 6 and Figure 7 demonstrate that given the correct circumstances it is possible to develop conditions where detrimental alignment of chamfers occurs. These conditions are heavily dependent on the drag torque present and contact flank. The consequence being extended engagement of the mechanism, resulting primarily from the restriction of engagement of hub chamfers with the sleeve. Further, the nature of variations in alignments of chamfers, gear chosen for engagement, and sleeve speed, and given that the examples shown here are general cases, suggest that delays in engagements could be further increased resulting from these variants.

The application of the same closed loop control method to the dry clutch model of the DCT presents a different, somewhat conflicting outcome. Though there is some perceptible delay for a negative chamfer alignment in Figure 7, these are more significant issue with the tip-on-tip alignment impeding engagement. Here triggering of the override control occurs for minor negative engagement but not when there is partial blocking engagement. Though it is possible to limit this misfiring through use of tolerances in the algorithm, there is sufficiently large range of variation in application of engagement that accurately trapping all negative engagements of the synchroniser may not be possible.

The use of closed loop chamfer control of the DCT has demonstrated that it is possible to use a relatively simple control technique to first identify detrimental alignment during indexing and use drag torque to realign the mechanism and continue engagement. For wet clutches it was identified that the push backwards and reengagement added

significantly to the duration of the entire process. While for dry clutches results demonstrated that there is insufficient drag to rapidly realign the mechanism from the tip-on-tip alignment, with control not triggered for tip-on-tip alignment conditions, but rather triggered when minor negative conditions that do not sufficiently degrade engagement occur. Consequently, the introduction of closed loop control does not necessarily provide an adequate and reliable tool for ensuring repeatable successful engagement under all conditions.

The results of Figure 13 demonstrate the effect of the same external excitation on the indexing of hub chamfers with similar alignment conditions for a dry DCT. These results present a marked improvement over the wet clutch alignment results, with detrimental chamfer alignments being rapidly forced to advantageous conditions. The rate of engagement for advantageous alignments is increased as the excitation further adds to the torques acting on alignments, while detrimental alignment are rapidly forced to the advantageous alignment condition, tip-on-tip contact is also rapidly engaged. These results lead to the conclusion that the higher drag torque, and subsequent regeneration of slip in the cone clutch affect the indexing of the synchroniser with detrimental alignment of chamfers using this control mechanism.

In comparison of Figures 12 and 13 it is observed that under detrimental engagement conditions the excitation torque provided tends to halt sleeve displacement before forcing it backward over chamfer tips to re-engage with positive torque alignment. This indicates that the phase angle of initial response in the excitation tool may be critical to minimising successful engagement times, furthering the assertion that tuning such an excitation tool has the potential in improve engagement with detrimental alignments in the wet DCT

simulations. The impact is less for dry clutch DCTs as the sleeve aligns rapidly to continue positive engagement, but the wet clutch case in Figure 12 results engagement delay with high drag countering the introduced torque.

Table 3: Summary of simulation results, and comparison to open loop simulations

			Up shift synchronisation		Down shift synchronisation	
	Simulation	Chamfer alignment condition	Duration of engagement (ms)	Difference with open loop (ms)	Duration of engagement (ms)	Difference with open loop (ms)
Wet Clutch	Open loop	$\theta_H < \delta/2$	89.57	-	56.57	-
		$\theta_H = \delta/2$	83.09	-	57.89	-
		$\theta_H > \delta/2$	81.84	-	62.62	-
	Closed loop	$\theta_H < \delta/2$	101.49	11.92	56.52	-0.05
		$\theta_H = \delta/2$	83.03	-0.07	57.84	-0.05
		$\theta_H > \delta/2$	81.79	-0.05	73.28	10.65
	Control tool	$\theta_H < \delta/2$	86.05	-3.52	56.58	0.01
		$\theta_H = \delta/2$	82.54	-0.56	83.46	25.57
		$\theta_H > \delta/2$	83.93	2.09	76.51	13.89
Dry Clutch	Open loop	$\theta_H < \delta/2$	83.53	-	57.65	-
		$\theta_H = \delta/2$	86.80	-	60.02	-
		$\theta_H > \delta/2$	84.18	-	58.72	-
	Closed loop	$\theta_H < \delta/2$	83.53	0.00	57.65	0.00
		$\theta_H = \delta/2$	86.80	0.00	60.02	0.00
		$\theta_H > \delta/2$	92.37	8.19	67.04	8.32
	Control tool	$\theta_H < \delta/2$	80.58	-2.95	56.01	-1.64
		$\theta_H = \delta/2$	79.77	-7.03	54.14	-5.88
		$\theta_H > \delta/2$	79.06	-5.12	54.07	-4.66

5. Conclusions

In the study of synchroniser mechanism actuation in dual clutch transmission it was identified that the repeatability of the engagement process is detrimentally affected by the alignment of hub and sleeve chamfers. This results from a combination of different factors: (1) after unblocking the synchroniser ring the cone clutch is de-energised and the

capacity to maintain speed synchronisation is lost, (2) drag torque acting on the target gear, particularly in wet multi-plate clutches, increases the slip speed in the cone before chamfers on sleeve and target gear come in contact, and (3) depending of contact flank indexing torque can oppose both the regenerated slip and drag torques, thus the indexing torque must brake the regenerated slip speed and re-attain synchronisation before it can positively engage chamfers. This is observed as block-out, or partial block-out of the sleeve, resulting in delay in synchroniser engagement.

Closed loop control of sleeve displacement to overcome detrimental chamfer alignments and the introduction external excitation to rapidly increased the rate of engagements have both been used to demonstrate possible solutions to provide direct control of chamfer engagements with varying degrees of success. Closed loop control engagements targets only detrimental alignments but increases the duration of synchroniser engagements well above the uncontrolled case. Given the process of engagement use of closed loop control does not guarantee that there re-engaging sleeve will not encounter the same alignment issues. The use of external excitation to initiate realignment provides additional torque to the synchroniser to increase the rate of chamfer realignment of the synchroniser has been successful in providing direct control of issues in chamfer alignment without significantly increasing the duration of engagements for most cases. These results have also indicated that there are some limitations to the design of the chamfer alignment tool in terms of selection of magnitude of inertia change or spring stiffness.

References

[1] B Matthes, F Geunter, Dual Clutch Transmissions - Lessons Learnt and Future Potential, SAE Technical Paper. 2005-01-1021 (2005) 119-130.

[2] G Wagner. Application of transmission systems for different driveline configurations in passenger cars, SAE Technical Paper. 2001-01-0882 (2001).

[3] Z Sun, K Hebbale, Challenges and opportunities in automotive transmission control, 2005 AACC. (2005) 3284-3284-3289.

[4] Y Liu, D Qin, H Jiang, Y Zhang. A systematic model for dynamics and control of dual clutch transmissions, Journal of Mechanical Design. 131 (2009).

[5] M Kulkarni, T Shim, Y Zhang. Shift dynamics and control of dual-clutch transmissions, Mechanism and Machine Theory. 42 (2007) 168-182.

[6] M Goetz, Integrated Powertrain control for Twin Clutch Transmissions, (2005), PhD thesis, University of Leeds.

[7] M Goetz, M Levesley, D Crolla. Dynamics and control of gearshifts on twin-clutch transmission, Proc Instn Mech Engrs Part D: J Automobile Engineering. 219 (2005) 951-963.

[8] G Lechner, H Naunheimer, Automotive Transmissions - Fundamentals, Selection, Design and Application, 1st ed., Springer-Verlag, Germany, 1999.

[9] RJ Socin, LK Walters. Manual transmission synchronizers, SAE Technical Paper. 680008 (1968).

[10] H Hoshino, Analysis on synchronisation mechanism of transmission, SAE World Congress & Exhibition, Session: Transmission and Driveline Systems. 1999-01-0734 (1999).

[11] D Kelly, C Kent, Gear shift quality improvement in manual transmissions using dynamic modelling, FISITA World Congress, Paper Number: F2000A126 (2000).

[12] J Kim, S Park, C Seok, H Song, D Sung, C Lim, et al. Simulation of the shift force for a manual transmission, Proc Instn Mech Engrs Part D: J Automobile Engineering. 217 (2003) 573-581.

[13] Y Liu, C Tseng. Simulation and analysis of synchronisation and engagement on manual transmission gearbox, Int. J. Vehicle Design. 43 (2007) 200-220.

[14] L Lovas, D Play, J Marialigeti, J Rigal. Mechanical behaviour simulation for synchromesh mechanism improvements, Proc Instn Mech Engrs Part D: J Automobile Engineering. 220 (2006) 919-945.

[15] B Paffoni, R Progri, R Gras. The mixed phase of gearbox synchromesh operation, Proc Instn Mech Engrs: Part J: J Engineering Tribology. 214 (2000) 157:165.

[16] ST Razzacki, J Hottenstein, Synchroniser design and development for dual clutch transmission (DCT), SAE World Congress & Exhibition, Session: Transmission and Drivelines (Part 2 of 8) Components. Paper Number: 2007-01-0114 (2007).

[17] PD Walker, N Zhang, R Tamba, S Fitzgerald, Synchroniser modelling with application specific to the dual clutch transmission, 13th Asia Pacific Vibration Conference. Paper number: 088, (2009).

[18] PD Walker, N Zhang, R Tamba, S Fitzgerald. Simulation of drag torque affecting synchronisers in a dual clutch transmission, JJIAM. Doi: 10.1007/s13160-011-0030-4 (2011).

[19] C Changenet, X Oviedo-Marlot, P Velex. Power loss predictions in geared transmissions using thermal networks: application to a six speed manual gearbox, Transactions of the American Society of Mechanical Engineers. 128 (2006) 618-625.

[20] NE Anderson, SH Loewenthal, Spur gear system efficiency at part and full load, NASA Technical Paper 1622. (1980).

[21] J Wheals, A Turner, K Ramsay, A O'Neil, J Bennett, H Fang. Double clutch transmission (DCT) using multiplexed linear actuation technology and dry clutches for high efficiency and low cost, SAE Technical Paper. 2007-01-1096 (2007).

[22] G Lucente, M Montanari, C Rossi. Modelling of an automated manual transmission system, Mechatronics. 17 (2007) 73-91.

[23] A Szadkowski, Shiftability and shift quality issues in clutch-transmission systems, SAE Technical Paper, Paper number: 912697 (1991).

[24] E M'Ewen. The theory of gear changing, Proc Instn Mech Engrs. (1948) 30-40.

[25] C Certez, O Scherf, K Stutzer, R Schierhorn, D Kelly. Wet or Dry Clutches for Dual Clutch Transmissions, FISITA World Congress and Exhibition 2004. F2004F136 (2004).

[26] J Stringer, Hydraulic systems analysis, an introduction, 1st ed., Macmillan Press Ltd, London, UK, 1976.

[27] FD Norvelle, Electrohydraulic control systems, 1st ed., Prentice Hall, USA, 2000.

[28] ND Manring, Hydraulic control systems, 1st ed., John Wiley & Sons, USA, 2005.

[29] M Koenig, D Firth, M Buchanan, Method for controlling the positioning of the synchronizers of a dual clutch transmission, US Patent (2004).

[30] SS Rao, Mechanical Vibrations, 1st ed., Addison-Wesley Publishing Co. USA, 1986

Appendix A – Hydraulic control system model

To develop the pressure model of the two hydraulic cylinders presented in Figure 4, begin with the differential equation of a compressible fluid and apply popular hydraulic theory found in [26-28].

$$Q = \frac{V}{\beta}\frac{dP}{dt} \tag{A.1}$$

Arranged to make pressure the subject

$$\int dP = \int \frac{Q \cdot \beta}{V} dt \tag{A.2}$$

With motion of the sleeve the volume of the cylinder will change, thus volume is not constant, or:

$$\int dP = \int \frac{Q \cdot \beta}{V_0 + dV} dt \tag{A.3}$$

It is assumed that the bulk modulus, β, is constant, so the relevant flow rates are required for inflow from the orifice, rate of change of cylinder, and leak flow out of the control volume. Q is therefore:

$$Q = Q_{Orifice} + Q_{Volume} + Q_{Leak} \tag{A.4}$$

Or, based on equations for sharp edged orifice and annular orifice presented in Stringer [26], and the rate of change in volume of the cylinder:

$$Q = C_D \pi \frac{D_{CV1}^{\ 2}}{4} \sqrt{P_S - P_{CV1}} - A_S \frac{dX_S}{dt} - C_D \pi D_S c_{RS} \sqrt{P_{CV1} - P_{EX}} \tag{A.5}$$

Equation A.5 is then substituted into equation A.3 to give Equations A.6 and A.7. Note that the sign difference for the volume rate of change is required as the piston heads move in opposing directions for the two cylinders:

$$P_{CV1} = \int \frac{\beta}{V_0 + dV} \left(C_D \pi \frac{D_{CV1}{}^2}{4} \sqrt{P_S - P_{CV1}} - A_S \frac{dX_S}{dt} - C_D \pi D_S c_{RS} \sqrt{P_{CV1} - P_{EX}} \right) dt \qquad \text{(A.6)}$$

$$P_{CV2} = \int \frac{\beta}{V_0 + dV} \left(C_D \pi \frac{D_{CV2}{}^2}{4} \sqrt{P_S - P_{CV2}} + A_S \frac{dX_S}{dt} - C_D \pi D_S c_{RS} \sqrt{P_{CV2} - P_{EX}} \right) dt \qquad \text{(A.7)}$$

List of Figure Captions

Figure 11: Example model of Inertia change system

Figure 12: Synchroniser engagement using excited hub indexing for wet clutches, fourth gear is synchronised with third gear engaged (top) and fifth gear engaged (bottom)

Figure 13: Synchroniser engagement using excited hub indexing for dry clutch DCT, fourth gear is synchronised with third gear engaged (top) and fifth gear engaged (bottom)

List of Table Captions